Oligofluorene–Thiophene Derivatives as High-Performance Semiconductors for Organic Thin Film Transistors

Hong Meng,[†] Jie Zheng,[‡] Andrew J. Lovinger,[§] Bo-Cheng Wang,[||]
P. Gregory Van Patten,[‡] and Zhenan Bao*,[§]

*Department of Chemistry and Biochemistry, University of California,
Los Angeles, California 90095, Department of Chemistry & Biochemistry, Ohio University,
Athens, Ohio 45701-2979, Bell Laboratories, Lucent Technologies, 600 Mountain Avenue,
Murray Hill, New Jersey 07974, and Department of Chemistry, Tamkang University,
151 Ying-Chuan Road, Tamsui, Taiwan 251*

A series of alkyl chain end-capped oligofluorene–thiophenes have been prepared with high yields using Suzuki or Stille coupling reactions. The electronic and optical properties of the thin films deposited at different substrate temperatures have been investigated. Morphological studies using transmission electron microscopy (TEM) revealed well-interconnected microcrystalline domains in these thin films. X-ray diffraction measurements of the vacuum-evaporated films showed enhanced crystalline order with increasing substrate deposition temperature. Thermal analysis as well as electrochemical measurements of the materials indicated that the new oligomers have high thermal and oxidative stability. Highly ordered polycrystalline vacuum-evaporated films with charge carrier mobility as high as 0.12 cm^2 V^{-1} s^{-1} have been achieved with 5,5′-bis(7-hexyl-9H-fluoren-2-yl)-2,2′-bithiophene (**DHFTTF**). Thin film field-effect transistor (TFT) devices made from these materials showed remarkable stability even after UV (366 nm) irradiation for more than 48 h in air. The semiconductors exhibit high on/off ratios (up to 10^5) and no significant decrease in mobility and on/off ratio over several months in air with exposure to ambient light. Finally, bright emission colors from greenish yellow to orange-red were observed in this new series of oligomer solid films excited with UV light (366 nm). In addition, a comparative study of the newly synthesized oligomers with α,α′-dihexylsexithiophene (**DH6T**), one of the most widely investigated oligothiophenes, is presented. The current approach to the molecular design can be applied toward the rational design of new TFT materials.

Introduction

Conjugated oligomers have received broad interest recently in academic as well as in industrial research communities.[1] The ease in obtaining compounds with high-purity and well-defined structures renders them promising active materials in thin film semiconductor devices such as organic light-emitting diodes (OLEDs),[2] organic field-effect transistors (OFETs),[3] solar cells,[4] nonlinear optical devices,[5] and waveguides.[6] They have also been used as model compounds of the corresponding conjugated polymers for structure–property relationship investigations.[7]

Organic thin-film transistors (TFTs) have been fabricated with several different semiconductors. Charge carrier mobilities on the order of 0.1 cm^2 V^{-1} s^{-1}, similar to those of amorphous Si transistors, have been achieved.[3] Among all investigated organic semiconductors, regio-

* Corresponding author. Phone: 908-582-4716. Fax: 908-582-4868. E-mail: zbao@lucent.com.
† University of California.
‡ Ohio University.
§ Lucent Technologies.
|| Tamkang University.

(1) (a) Barbarella, G.; Favaretto, L.; Sotgiu, G.; Zambianchi, M.; Bongini, A.; Arbizzani, C.; Mastragostino, M.; Anni, M.; Gigli, G.; Cingolani, R. *J. Am. Chem. Soc.* **2000**, 122, 11971. (b) Ho, H. A.; Brisset, H.; Elandaloussi, E. H.; Frere, P.; Roncali, J. *Adv. Mater.* **1996**, 8, 990. (c) Hicks, R. G.; Nodwell, M. B. *J. Am. Chem. Soc.* **2000**, 122, 6746.

(2) (a) Belletete, M.; Beaupre, S.; Bouchard, J.; Blondin, P.; Leclerc, M.; Durocher, G. *J. Phys. Chem. B* **2000**, 104, 9118. (b) Leclerc, M. *J. Polym. Sci., Polym. Chem.* **2001**, 39, 2867. (c) Mitschke, U.; Bauerle, P. *J. Mater. Chem.* **2000**, 10, 1471. (d) Noda, T.; Ogawa, H.; Noma, N.; Shirota, Y. *J. Mater. Chem.* **1999**, 9, 2177. (e) Heidenhain, S. B.; Sakamoto, Y.; Suzuki, T.; Miura, A.; Fujikawa, H.; Mori, T.; Tokito, S.; Taga, Y. *J. Am. Chem. Soc.* **2000**, 122, 10240.

(3) (a) Horowitz, G. *Adv. Mater.* **1998**, 10, 365. (b) Katz, H. E.; Lovinger, A. J.; Johnson, J.; Kloc, C.; Siegrist, T.; Li, W.; Lin, Y. Y.; Dodabalapur, A. *Nature* **2000**, 404, 478. (c) Bao, Z.; Rogers, J. A.; Katz, H. E. *J. Mater. Chem.* **1999**, 9, 1895. (d) Dimitrakopoulos, C. D.; Mascaro, D. J. *IBM J. Res. Dev.* **2001**, 45, 11. (e) Klauk, H.; Jackson, T. N. *Solid State Technol.* **2000**, 43, 63. (f) Lin, Y.-Y.; Gundlach, D. J.; Nelson, S. F.; Jackson, T. N. *IEEE Trans. Electron Devices* **1997**, 44, 1325. (g) Li, X. C.; Sirringhaus, H.; Garnier, F.; Holmes, A. B.; Moratti, S. C.; Feeder, N.; Clegg, W.; Teat, S. J.; Friend, R. H. *J. Am. Chem. Soc.* **1998**, 120, 2206. (h) Meng, H.; Bao, Z.; Lovinger, A. J.; Wang, B.; Mujsce, A. M. *J. Am. Chem. Soc.* **2001**, 123, 9214.

(4) (a) Schmidt-Mende, L.; Fechtenkötter, A.; Müllen, K.; Moons, E.; Friend, R. H.; MacKenzie, J. D. *Science* **2001**, 293, 1119. (b) Schön, J. H.; Kloc, C.; Bucher, E.; Batlogg, B. *Nature* **2000**, 403, 6768.

(5) (a) LutherDavies B.; Samoc, M. *Curr. Opin. Solid State Mater.* **1997**, 2, 213. (b) Blanchard, P.; Raimundo, J. M.; Roncali, J. *Synth. Met.* **2001**, 119, 527.

(6) Kozlov, V. G.; Parthasarathy, G.; Burrows, P. E.; Khalfin, V. B.; Wang, J.; Chou, S. Y.; Forrest, S. R. *IEEE J. Quantum Electron.* **2000**, 36, 18.

(7) Katz, H. E.; Bao, Z.; Gilat, S. L. *Acc. Chem. Res.* **2001**, 34, 359.

**Scheme 1. Chemical Structures of
α,α′-Dihexylsexithiophene (DH6T) and
Dihexyl-oligofluorene−thiophenes**
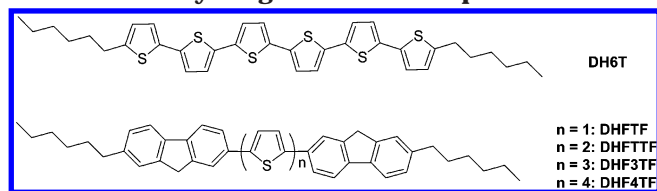
regular poly(3-alkylthiophene)s, oligothiophene derivatives, and fused aromatic compounds such as pentacene and tetracene have shown the most promising performance.[3] Most of these p-channel semiconductors [hole being the major charge carrier] possess relatively low band gap and a high-energy highest occupied molecular orbital (HOMO) level. Therefore, they are easily oxidized, which results in poor device stability, making them unsuitable for practical electronic circuit applications.[7] To address this problem, design and synthesis of organic semiconductors with high charge carrier mobility as well as good stability is desirable. It is generally accepted that the charge carrier transport in organic OFETs is dominated by the hopping mechanism.[8] To achieve good performance of OFETs, highly ordered thin films with large interconnected polycrystalline grains are necessary. In addition, to facilitate the charge injection process, the HOMO energy level of the material should match well with the work function of the source or drain electrodes.[9] High charge carrier mobility fluorescent organic semiconductors are also interesting for electrically injected lasers.[10]

Thiophene oligomers are promising charge transport semiconductors. The ease in chemical modification of their structures can potentially allow us to fine-tune their optical and electronic properties. One of the most widely investigated oligothiophenes is α,α′-dihexylsexithiophene (**DH6T**)[11] (Scheme 1), which has a reported field-effect mobility of 0.05 cm^2 V^{-1} s^{-1} with an on/off ratio up to 10^6. However, a significant drawback of oligothiophenes are their low fluorescence and poor stability, especially in solid states.[12] On the other hand, oligofluorenes show much higher fluorescent efficiency and better stability due to their rigid structure and lower HOMO level compared to thiophene oligomers.[2] These materials have been used for LEDs,[2] and recently TFTs from fluorene-containing polymers have been reported.[13] However, high mobility was obtained only after the polymer had been annealed in the liquid-crystalline (LC) phase aligned with a rubbed polyimide surface to form a monocrystalline domain.[13]

Our previous results have shown that high field-effect mobility (>0.1 cm^2 V^{-1} s^{-1}) and stable FETs can be achieved with 5,5′-bis(7-hexyl-9*H*-fluoren-2-yl)-2,2′-bithiophene (**DHFTTF**).[3h] By adjusting the conjugation length of the thiophene units between the two fluorenes, it is possible to fine-tune the energy level and emission color of the resulting materials. In this work, we continue our effort to design a new series of conjugated oligomers combining the properties of oligofluorenes and oligothiophenes. To facilitate π−π* stacking and increase the solubility of these oligomers in organic solvents, alkyl chains are attached to the 7-position of the two fluorenes (Scheme 1). This is in contrast to the polyfluorenes and oligofluorenes used for light-emitting diodes, in which alkyl chains are substituted at the methylene linkage (9-position) of fluorene to improve its solubility and decrease aggregation.[14] To fine-tune the optical and electronic properties, oligothiophenes ranging from one to four moieties were introduced in conjugated linkage with two fluorene units. In the following sections, detailed synthesis and characterization of these new oligomers and their application in TFTs have been presented. We discuss these results in terms of conjugation length, molecular stability, optical properties, and the device performance. This study may help us to understand the structural relationship of the materials and provide a useful way for the rational design of new transistor materials.

Results and Discussions

Synthesis. Scheme 2 outlines the synthetic steps to prepare fluorene−thiophene oligomers. The syntheses of **DHFTF**, **DHFTTF**, and **DHF3TF** involved Suzuki coupling reactions[15] between the substituted 2-hexyl-fluorene pinacolato boronic ester **3** and the corresponding dibromo-substituted mono-, bi-, and terthiophene units, respectively. The boronic ester was synthesized via direct cross-coupling between the substituted bromo-fluorene and bis(pinacolato)diboron. This reaction has been reported to tolerate various functional groups.[16] **DHF4TF** was synthesized using the Stille coupling reaction[17] between 5,5′-bis-tributylstananyl-2,2′-bithiophene and 2-bromo-5-(7-hexyl-9*H*-fluoren-2-yl)thiophene (**5**). The results from elemental analysis and ^{1}H NMR and mass spectrometric (MS) analysis confirmed that the synthesized compounds have the predicted chemical structures. All the oligomer materials are moderately soluble in hot dichlorobenzene and chloroform to allow NMR measurements.

Thermal Properties. Thermogravimetric analysis (TGA) reveals that the oligomers are thermally stable, with the onset of decomposition temperatures at 400 °C under nitrogen atmosphere. In contrast, oligothiophene-

(8) (a) Sirringhaus, H.; Tessler, N.; Friend, R. H. *Science* **1998**, *280*, 1741. (b) Katz, H. E.; Lovinger, A. J.; Johnson, J.; Kloc, C.; Siegrist, T.; Li, W.; Lin, Y. Y.; Dodabalapur, A. *Nature* **2000**, *404*, 478. (c) Lin, Y.-Y.; Gundlach, D. J.; Nelson, S. F.; Jackson, T. N. *IEEE Trans. Electron Devices* **1997**, *44*, 1325. (d) Katz, H. E.; Bao, Z. *J. Phys. Chem. B* **2000**, *104*, 671. (e) Horowitz, G.; Hajlaoui, M. E. *Adv. Mater.* **2000**, *12*, 1046.
(9) Katz, H. E.; Bao, Z. *J. Phys. Chem. B* **2000**, *104*, 671.
(10) Schön, J. H.; Dodabalapur, A.; Kloc, Ch.; Batlogg, B. *Science* **2000**, *290*, 963.
(11) Facchetti, A.; Deng, Y.; Wang, A. C.; Koide, Y.; Sirringhaus, H.; Marks, T. J.; Friend, R. H. *Angew. Chem., Int. Ed.* **2000**, *39*, 4547.
(12) Yu, W.; Meng, H.; Pei, J.; Huang, W. *J. Am. Chem. Soc.* **1998**, *120*, 11808.
(13) Sirringhaus, H.; Wilson, R. J.; Friend, R. H.; Inbasekaran, M.; Wu, W.; Woo, E. P.; Grell, M.; Bradley, D. D. C. *Appl. Phys. Lett.* **2000**, *77*, 406.

(14) (a) Sirringhaus, H.; Kawase, T.; Friend, R. H.; Shimoda, T.; Inbasekaran, M.; Wu, W.; Woo, E. P. *Science* **2000**, *290*, 2123. (b) Klarner, G.; Davey, M. H.; Chen, W. D.; Scott, J. C.; Miller, R. D. *Adv. Mater.* **1998**, *10*, 993. (c) Setayesh, S.; Grimsdale, A. C.; Weil, T.; Enkelmann, V.; Mullen, K.; Meghdadi, F.; List, E. J. W.; Leising, G. *J. Am. Chem. Soc.* **2001**, *123*, 946. (d) Miteva, T.; Meisel, A.; Knoll, W.; Nothofer, H. G.; Scherf, U.; Muller, D. C.; Meerholz, K.; Yasuda, A.; Neher, D. *Adv. Mater.* **2000**, *13*, 565.
(15) Miyaura, N.; Suzuki, A. *Chem. Rev.* **1995**, *95*, 2457−2483.
(16) Ishiyama, T.; Murata, M.; Miyaura, N. *J. Org. Chem.* **1995**, *60*, 7508−7510.
(17) Bao, Z.; Chan, W. K.; Yu, L. *J. Am. Chem. Soc.* **1995**, *117*, 12426.

Scheme 2. Synthetic Routes of Oligofluorene−thiophenes
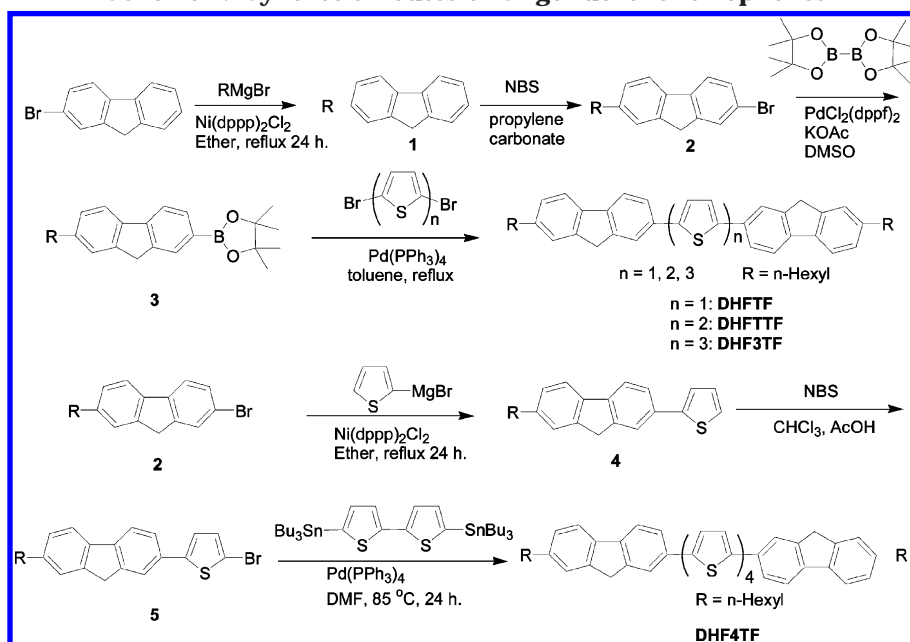
based **DH6T** decomposes at 320 °C under similar conditions.[11] The thermal phase transitions of these compounds were analyzed by differential scanning calorimetry (DSC). As expected, the increase of the number of thiophene rings results in the increase of the phase transition temperature. The first major phase transition temperature for **DHFTF**, **DHFTTF**, **DHF3TF**, and **DHF4TF** is 332, 381, 390, and 395 °C, respectively. The corresponding crystallization temperature upon cooling is 322, 368, 381, and 370 °C, for **DHFTF**, **DHFTTF**, **DHF3TF**, and **DHF4TF**, respectively. The thermal transition was clearly observed in **DHFTF**. Figure 1 illustrates the heating process, which includes a phase transition temperature at 332 °C followed by perhaps the liquid crystal to isotropic transition (melting point) at 393 °C (birefringence was observed under a cross-polarized microscope when the sample was heated above 320 °C).

The upper cooling curve shows a slight displacement of the transitions at 382 and 322 °C due to supercooling.[18] For the other three oligomers, the second phase transition temperature (melting point) was difficult to determine accurately since they started to decompose during melting. All the materials are crystalline and exhibit clear endothermic peaks during the first and also second heating cycles. The fact that all the materials form crystalline phases indicates that well-ordered films
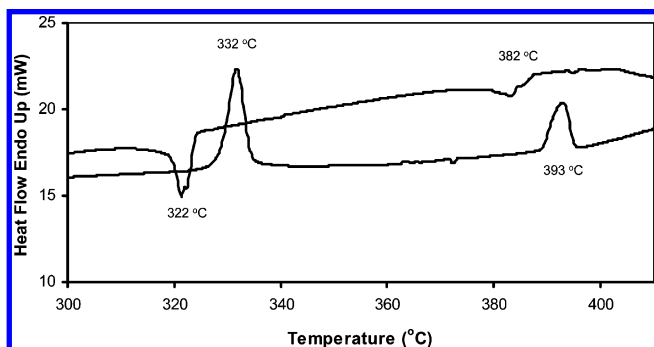
may be formed during thermal evaporation processes. In addition, compared with **DH6T**, which showed crystalline phase transition states with the phase transition temperature at 290, 298, and 318 °C, the new oligomers showed significantly higher phase transition temperatures.

Transmission Electron Microscopy. Thin films of the oligomeric materials deposited by vacuum evaporation at different substrate temperatures were examined by transmission electron microscopy (TEM) and electron diffraction. Typical morphologies of our oligomeric materials are seen in Figure 2. In general, all new oligomers showed well-connected crystallites similar to those of **DH6T**. However, unlike **DH6T** and other oligothiophenes, in which the increase of the substrate temperature may eventually cause discontinuities at the grain boundaries, resulting in lower field-effect mobilities,[11,19,20] the new oligomers have well-connected grains even as the deposition temperature is increased substantially. At room temperature **DHFTF** [Figure 2a] consists of irregular but well-connected grains in the 100-nm range. When the substrate deposition temperature is raised to 100 °C, the morphology shows a distinct improvement with the introduction of crystallographic faceting and distinct screw dislocations. At 140 °C, the crystals are now large, flat lamellae with dimensions well into the micrometer range. The reason for the charge carrier mobility not being improved significantly for **DHFTF** may be that there is a significant energy barrier between crystals for charge transport because of the fewer nucleation events in these thin films at high temperatures.

For **DHFTTF** [Figure 2b], a similar irregular granular morphology is obtained at 25 °C, which improves in average size to ca. 250 nm at 100 °C. Deposition at even

Figure 1. Differential scanning calorimetry (DSC) thermograms of **DHFTF**.

(18) Destri, S.; Khotina, I. A.; Porzio, W. *Macromolecules* **1998**, *31*, 1079.
(19) Lovinger, A. J.; Davis, D. D.; Dodabalapur, A.; Katz, H. E. *Chem. Mater.* **1996**, *8*, 2836.
(20) Garnier, F.; Yassar, A.; Hajlaoui, R.; Horowitz, G.; Deloffre, F.; Servet, B.; Ries, S.; Alnot, P. *J. Am. Chem. Soc.* **1993**, *115*, 8716.
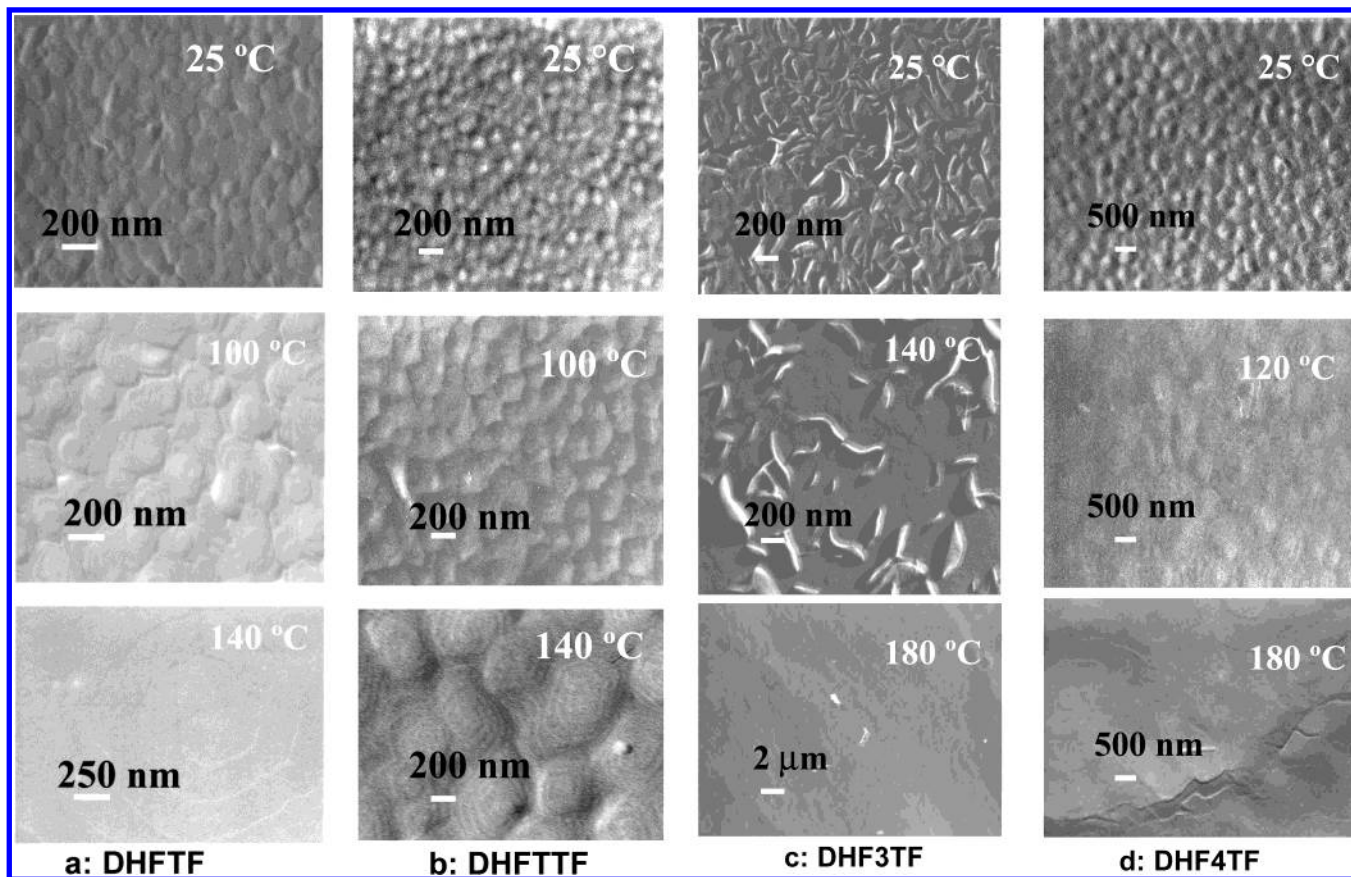
Figure 2. Transmission electron micrographs of the films deposited at different temperatures: (a) **DHFTF**; (b) **DHFTTF**; (c) **DHF3TF**; (d) **DHF4TF**.

higher temperatures (140 °C) yields much improved crystals ca. 500 nm in width, with clear faceting, screw dislocations, and terraces. An important point to note is that the crystals are seen to be well-connected, and this accounts for the observed increase in mobility at these high deposition temperatures.

In the case of **DHF3TF**, the morphology is different [see Figure 2c]. At ambient deposition temperature the crystals are rodlike with very poor connectivity. A mixture of rodlike (probably edge-on lamellae) and flat crystals is obtained when the substrate is kept at 140 °C, but the long-range continuity is still poor. Its morphology probably explains the very low mobilities measured under these conditions. Only at the highest temperature of 180 °C are large, well-connected crystalline aggregates obtained, and at these temperatures charge carrier mobility reaches a reasonable value ($0.025 \text{ cm}^2 \text{ V}^{-1} \text{ s}^{-1}$).

Finally, for **DHF4TF** [Figure 2d], the structure at room temperature is again nodular (ca. 80-nm diameter). The morphological improvement at 120 °C, evident in the multilayer terraces and increased crystalline sizes, is accompanied by enhanced mobility. At the highest temperature (180 °C), large (many micrometer) multilayer lamellae are obtained. Their good intercrystalline contacts ensure further increase in mobility. However, because intercrystalline boundaries can be thinner (sometimes a single lamella thick), failures do occur in some devices after a number of cycles.

X-ray Diffraction. The X-ray diffraction patterns of all oligomers are similar as shown Figure 3. Generally, all films showed high crystallinity. Preferred orientation
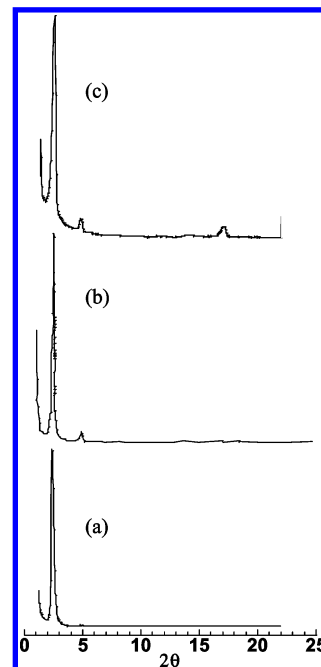

Figure 3. X-ray diffractograms of **DHFTTF** films prepared at T_D of (a) 25 °C and (b) 140 °C and (c) cast from chlorobenzene solution at T_D of 120 °C.

is clearly inferred through the dominance of peaks at 33–37 Å and the absence of strong peaks in the 3–5-Å regions seen in our X-ray diffractograms in the Bragg–Brentano geometry. The former spacing corresponds to the end-to-end packing of molecular chains (such as that of **DHFTTF** seen in the molecular model of Figure 4),
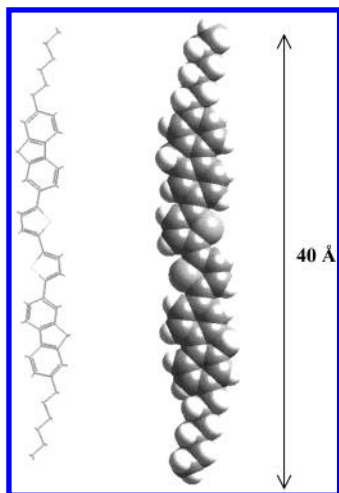
Figure 4. Molecular model of **DHFTTF**.

Table 1. Observed *d* Spacings from X-ray Diffraction Data Compared with Calculated Extended Chain Lengths

oligomer	extended chain lengths	observed *d* spacing
DHFTF	36 Å	33 Å
DHFTTF	40 Å	34−35 Å
DH3TF	44 Å	36−37 Å
DH4TF	48 Å	34 Å

with the latter to their side-by-side arrangement. These findings indicate an almost orthogonal deposition of molecules onto the substrate. However, some slight chain tilting must be present since the observed *d* spacings (Table 1) are smaller than the corresponding extended chain lengths. The tilting increases with oligomer length, but interestingly, the observed *d* spacings do not increase monotonically. The reason for the latter is not clear and would require synthesis of longer oligomers to probe any trends with the number of thiophene monomers. It is conceivable that an "odd−even effect" might also play a role here: as seen from the model of Figure 4, the alkyl end chains are inclined to opposite sides of the aromatic molecular cores for an even number of thiophene monomers, but would be on the same side for odd number (unless the fluorene units are rotated by 180°).

Figure 3 also shows the diffractogram at a high substrate deposition temperature (which does not display significant improvement over the already excellent preferred orientation), as well as the corresponding diffractogram for a solution deposited film. For the film deposited from solution, there are clear signs of less than perfect orientation: there are additional reflections that do not correspond to multiple orders of the primary 35-Å peak (e.g., one at 5.2 Å arising from the side-by-side packing of chains).

Electronic and Optical Properties. The UV−vis absorption and photoluminescence (PL) spectra of the vacuum-evaporated oligomer thin films deposited at substrate temperature of about 25 °C are depicted in Figure 5. Two absorption peaks (λ_{max}) are observed for each oligomer. The one at longer wavelength is around 325−375 nm corresponding to the $\pi-\pi^*$ transition of the conjugated oligomer, while the shorter wavelength band (λ_{max} 250−285 nm) originates from the electronic transition of the individual aromatic units. The general

trend of the absorption spectra is the red shift of the $\pi-\pi^*$ transition band with increasing number of thiophene rings. The HOMO−LUMO energy gaps (summarized in Table 2), determined by extrapolating the long-wavelength absorption edge, decreases with the increase of π conjugation length. All films showed blue shift of the main absorption peaks compared to their diluted chloroform solutions, which suggests an *H*-aggregate formation by analogy with previous work.[21]

To compare the relative photoluminescent efficiencies of the oligomers, they were measured in diluted chloroform solutions using perylene in cyclohexane as a reference (100%). In solution, the relative fluorescent quantum efficiencies (QE) of **DHFTF**, **DHFTTF**, **DHF3TF**, and **DHF4TF** are 56%, 25%, 21%, and 19%, respectively. The results indicate that the QE of the oligomers decreases with the increasing of the number of the thiophene moieties. The same trend is also observed in the solid state (both in powder and thin films), as qualitatively shown in Figure 5 (photo inset). Interestingly, **DH6T** shows relatively high QE in solution, which becomes very weak in the solid state (due to Davydov splitting).[20]

The enhanced PL efficiency in the solid state of these oligomers results from the fluorene units or the lower number of thiophene rings in the main conjugated backbone.[22] We also measured the QE of α,α′-dihexyl-quaterthiophene (**DH4T**) under similar conditions. In solution, the QE of **DH4T** is 17%, which is lower than that of **DH6T** (28%), whereas in the solid state **DH4T** shows qualitatively higher fluorescence.

Electrochemistry. To understand the charge transport properties and the stability of the materials, electrochemistry measurements of the thin films were carried out. Table 2 summarizes the cyclic voltammetric (CV) data along with band gaps determined from UV−vis spectra as a comparison. All compounds showed two partially reversible oxidation waves, yielding radical cation and dication species as well as one partially reversible reduction wave to afford the radical anions.[23] The increased conjugation (from **DHFTF** to **DHF4TF**) results in a decrease of the oxidation potentials and the reduction potentials. Similar behavior has been observed in **DH6T**, which also showed two oxidation waves, but at much lower potentials compared to oligofluorene−thiophenes (Table 2).[23] The relative high oxidation potentials of our oligomers resulted in better oxidation stability of the materials. The HOMO and LUMO levels of the materials were determined using the onset positions of the oxidation and reduction processes according to other literature reports.[23] The band gap derived from this method showed good agreement with those obtained from the UV−vis absorption spectra. The determined HOMO levels of the oligomers are in the range of −5.39 to −5.06 eV, which match well with the work function of gold metal.

FET Device Performance. Field-effect transistors were made both in bottom contact (semiconductor

(21) Nüesh, F.; Grätzel, M. *Chem. Phys.* **1995**, *193*, 1.
(22) Liu, B.; Yu, W.; Lai, Y.; Huang, W. *Macromolecules* **2000**, *33*, 8945.
(23) (a) de Leeuw, D. M.; Simenon, M. M. J.; Brown, A. R.; Einerhand, R. E. F. *Synth. Met.* **1997**, *87*, 53. (b) Cervini, R.; Li, X.-C.; Spencer, W. C.; Holmes, A. B.; Moratti, S. C.; Friend, R. H. *Synth. Met.* **1997**, *84*, 359. (c) Nessakh, B.; Horowitz, G.; Garnier, F.; Deloffre, F.; Srivastava, P.; Yassar, A. *J. Electroanal. Chem.* **1995**, *399*, 97.
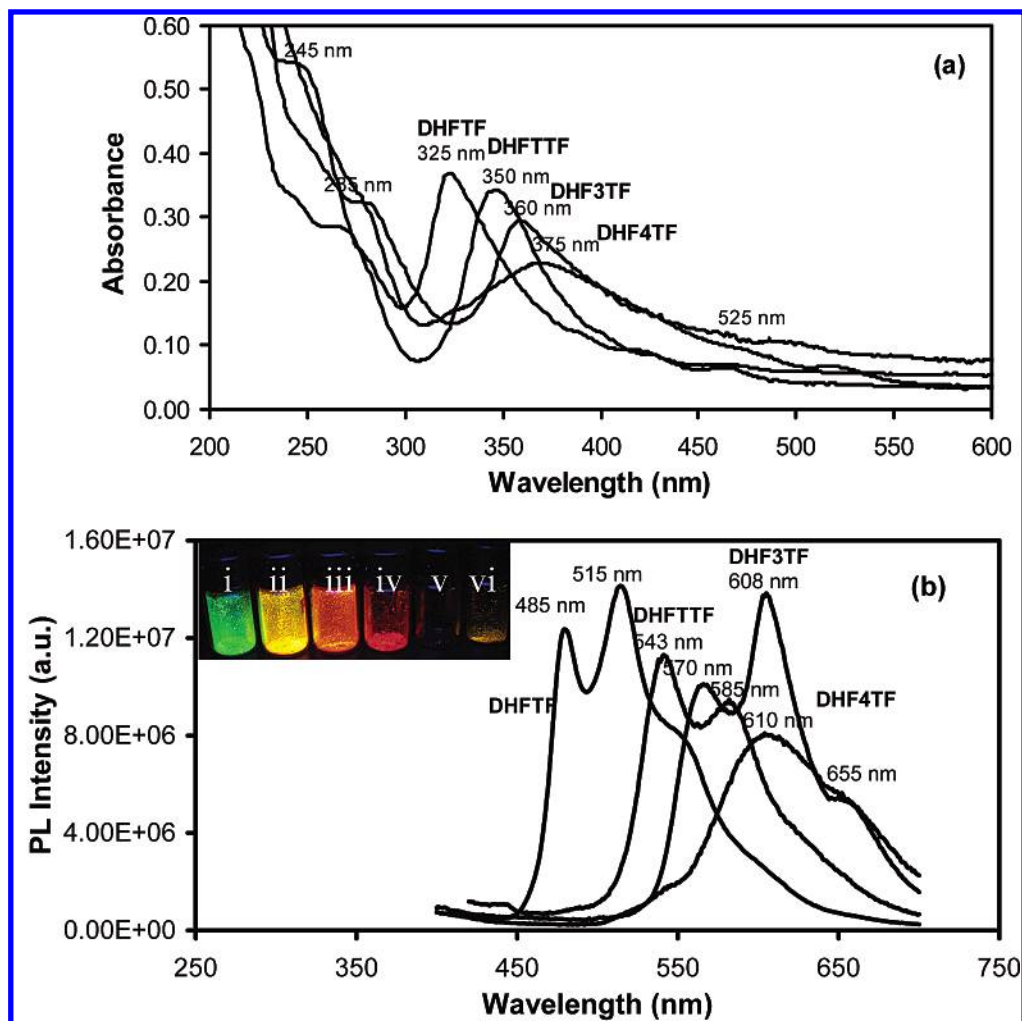
Figure 5. (a) UV−vis and (b) PL spectra of the oligomer thin films deposited at RT. (Inserted photo shows corresponding powder emission color of the oligomers excited at 366 nm by a UV lamp. (i) **DHFTF**, (ii) **DHFTTF**, (iii) **DHF3TF**, (iv) **DHF4TF**, (v) **DH6T**, and (vi) **DH4T**. No or very weak emission was observed from (v) **DH6T** or (vi) **DH4T**, respectively.

Table 2. HOMO and LUMO Energy Levels and Band Gaps Determined from the Optical and Electrochemical Measurements of the Oligomers

oligomer	oxidation E_{pa}/E_{pc} (V)[a]	reduction E_{pc}/E_{pa} (V)[a]	reduction E^{onset} (V) LUMO eV	oxidation E^{onset} (V) HOMO eV	λ_{onset} E_g (eV) UV[b]	E_g (eV) Echem[c]
DHFTF	+1.15/+0.82	not available	−1.97	+0.95	448 nm	
	+1.43/+0.98		−2.47	−5.39	2.77	2.92
DHFTTF	+1.13/+0.82		−1.91	+0.92	468 nm	
	+1.33/+1.21	−2.46/−2.13	−2.53	−5.36	2.65	2.83
DHF3TF	+0.89/+0.79		−1.79	+0.64	536 nm	
	+1.26/+0.96	−2.13/−2.00	−2.65	−5.08	2.31	2.43
DHF4TF	+0.82/+0.75	−2.04/−1.96	−1.64	+0.62	550 nm	
	+1.09/+1.02		−2.80	−5.06	2.25	2.26
DH6T	+0.70/+0.63	−2.03/−1.92	−1.81	+0.51	511 nm	2.32
	+1.10/+0.77		−2.63	−4.95	2.42	
Au	work functions: Au(110), −5.37 eV; Au(100), −5.47 eV; Au(111), −5.31 eV					

[a] Peak potentials of cathodic (E_{pc}) and anodic (E_{pa}) peaks, respectively. [b] HOMO−LUMO gap (E_g) measured according to the onset of UV absorption of the deposited films ($E_g = 1240/\lambda_{onset}$ eV). [c] HOMO−LUMO gap (E_g) according to the equation reported by de Leeuw et al.[23]

deposited above the drain and source electrodes) and top contact (drain and source electrodes deposited above the semiconducting material) device geometries. The substrate temperatures during deposition (T_D) for all oligomers were in the range of 25−180 °C. The device performance was measured in air and the results are shown in Table 3.

All devices prepared using the bottom contact geometry, in general, showed lower charge carrier mobility than those using the top contact geometry. In some cases, the bottom contact devices did not show any transistor activities. Similar observations have been reported for other FET materials.[3] This was attributed to the small charge injection areas and poor nucleation

Table 3. Field-Effect Mobilities[a] and On/Off Ratios[b] of the Oligomers Deposited at Different Substrate Temperatures (T_D)

		T_D = 25 °C		T_D = 100 °C		T_D = 140 °C		T_D = 180 °C	
oligomer	FET structure	μ cm^2 V^{-1} s^{-1}	on/off ratio	μ cm^2 V^{-1} s^{-1}	on/off ratio	μ cm^2 V^{-1} s^{-1}	on/off ratio	μ cm^2 V^{-1} s^{-1}	on/off ratio
DHFTF	top	5.1×10^{-3}	2×10^3	4.7×10^{-3}	2×10^3	5.9×10^{-3}	2×10^3	1.2×10^{-2}	1×10^3
	bottom	6.3×10^{-4}	5×10^2	1.0×10^{-3}	6×10^2	1.5×10^{-3}	3×10^2	2.0×10^{-3}	5×10^2
DHFTTF	top	2.5×10^{-2}	2×10^3	5.6×10^{-2}	2×10^3	1.1×10^{-1}	1×10^5	1.4×10^{-1}	2×10^4
	bottom	4.0×10^{-3}	1×10^3	1.2×10^{-2}	1×10^3	6.0×10^{-2}	2×10^4		
DHF3TF	top	not active	not active	3.4×10^{-4}	50	5.4×10^{-3}	1×10^3	2.5×10^{-2}	1×10^2
	bottom	not active	not active	not active	not active				
DHF4TF	top	7.6E−4	1×10^2	1.4E−2	1×10^2	1.7×10^{-2}	3×10^2	2.3×10^{-2}	1×10^2
	bottom	not active	not active	not active	not active	2.4×10^{-4}	4×10^1		

[a] Mobility is calculated using currents from the saturation regions. [b] On/off ratio is calculated for gate voltages from 0 to −100 V.
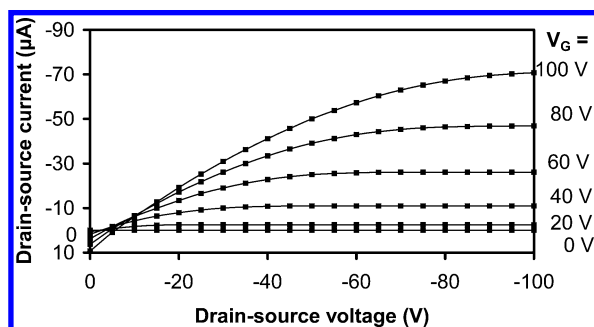

Figure 6. Drain-source current (I_{DS}) vs drain-source voltage (V_{DS}) characteristic of **DHFTTF** at different gate voltages prepared at a substrate temperature of 140 °C with channel length $L = 280$ μm and channel width $W = 4$ mm.

Figure 7. FET top-contact mode charge mobilities of the oligomers at different substrate temperatures.

of the organic semiconductor vapor on the electrodes in the bottom contact geometry. The films deposited in the gold electrode region appeared rather nonuniform under an optical microscope.

Figure 6 shows the typical FET characteristic of a TFT made of **DHFTTF** deposited at $T_D = 140$ °C. All oligomers operated as p-channel transistors in air. The $I-V$ characteristics showed standard linear and saturation regions. The drain source current scales nicely with increasing gate voltages. For top-contact devices, the field-effect mobilities are generally higher for films deposited at higher substrate temperatures. This is related to better interconnection between crystals and larger crystallite sizes for films prepared at higher T_D, which was confirmed by X-ray diffraction patterns and transmission electron micrographs. A similar trend has been reported for other vacuum-evaporated oligomers.[3,7] The effect of substrate temperature during deposition on the charge carrier mobility can be easily seen in Figure 7.

The highest charge carrier mobility among the four oligomers was obtained with **DHFTTF**. **DHFTF** showed higher mobilities at lower deposition temperature (25 °C) than that of **DHF3TF** and **DHF4TF**. However, for films deposited at elevated substrate temperatures, the latter two oligomers showed higher mobilities than those of **DHFTF**. These results indicate that there may exist some relationship between the mobility, the conjugation length, and the deposition temperatures, but a wider range of materials would be needed to confirm the result. The lower on/off ratios of the **DHF3TF** and **DHF4TF** probably are due to their higher HOMO levels (easier to be oxidized) and higher sublimation temperatures, which may cause partial decomposition during deposition. However, the on/off ratio can often be
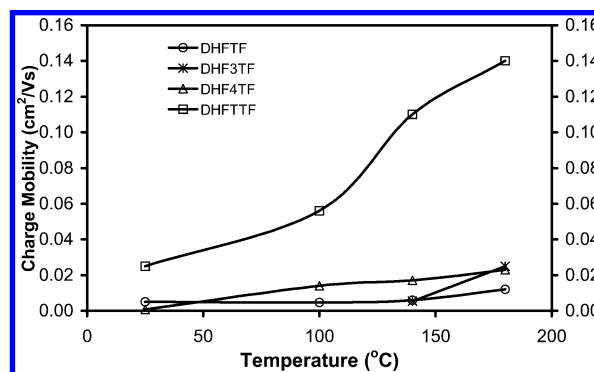
improved by dielectric surface treatment, repeated purification, and/or patterning of the semiconducting materials.[3,11,24]

Solution-Processable FET. By introduction of the alkyl end groups, the solubility of the oligomers is greatly improved. It is therefore possible to make solution-processable devices by casting from the oligomer solutions.[3] We tested thin films of **DHFTTF** cast from hot chloroform (1 mg/mL) or hot chlorobenzene (2 mg/mL) solutions. Uniform well-ordered films (X-ray diffraction pattern shown in Figure 3c) can be formed from chlorobenzene solution with measured charge carrier mobility in the range of $1.69-2.24 \times 10^{-3}$ cm^2 V^{-1} s^{-1}. These values are lower than those of the devices made from vacuum-evaporated films and reflect the somewhat poorer orientation of the former. The $I-V$ characteristic of a solution-cast FET is shown in Figure 8. Optimization of film deposition conditions will be required to achieve better performance.

Device Stability Test. To test the stability of the devices, transistors made of **DHFTTF** as the active layer were stored in air with exposure to ambient light in a regular lab environment without any encapsulation for several months with their mobilities and on/off ratios measured periodically. For accelerated testing, a device was exposed to a UV lamp (366 nm, 60 Hz, 0.16 A) for 48 h and tested. Exposure of the devices to air caused only slight changes of their mobilities and on/off ratios even after several thousand hours, while most of the other p-channel organic semiconductors show a much faster decrease in mobility and on/off ratio. The on/off ratio of the exposed device was still on the same order of magnitude as that of the freshly prepared device. The
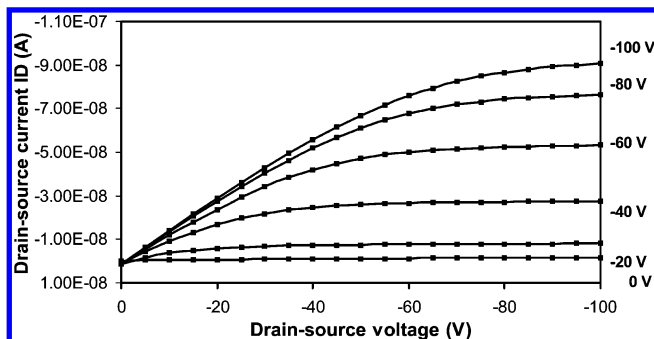
(24) Lovinger, A. J.; Katz, H. E.; Dodabalapur, A. *Chem. Mater.* **1998**, *10*, 3275.

Figure 8. I_{DS} vs V_{DS} characteristic of DHFTTF cast film at different gate voltages prepared from chlorobenzene solution with W/L = 1.
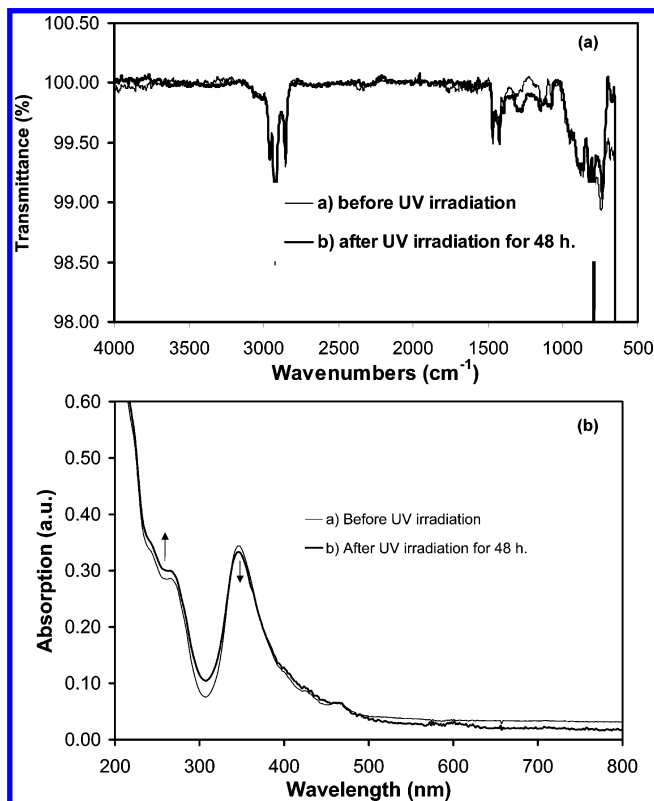

Figure 9. (a) FT-IR and (b) UV spectra of the thin films of **DHFTTF** before and after UV irradiation.

device, however, did show decreased charge mobility (10^{-4} cm^2 V^{-1} s^{-1}) after 24 h of UV exposure in air.

We also measured the FT-IR and UV−vis spectra of **DHFTTF** films exposed to UV light (366 nm, 60 Hz, 0.16 A) for 48 h in air. Figure 9 shows spectra of the thin film before and after UV-light exposure. To our surprise, the 9-position of fluorene did not show signs of photo-oxidation since no vibration peaks from the carbonyl functional group was observed in the FT-IR spectrum. The UV−vis spectrum did show slight changes in the peak absorption intensity, indicating that there may be partial loss of conjugation of the oligomer after 48 h of UV irradiation. This explains why the mobility is lower after UV irradiation, even though not much change has been observed. Compared with **DH6T** and polythiophenes, which decompose quickly (within hours) under UV light exposure, the fluorene-containing oligomers described here exhibited better oxidative stability.

Conclusion

In summary, we have successfully synthesized a series of oligofluorene−thiophenes. The HOMO energy levels of all the materials are in the range of 5.0−5.4 eV, which match well with the work function of the gold electrodes, favoring the charge injection of holes. High-mobility transistors are obtained when the films are deposited at elevated substrate temperatures. The introduction of end substituents favored the ordered arrangement of the molecules, which facilitates the charge transport through $\pi−\pi^*$ stacking of the molecules. These end groups also improve the material solubility so that solution-processable FETs can be fabricated. Studies of the FET mobility with different oligomer conjugation length indicate that there may exist some relationships between the mobility, the conjugation length, and the deposition temperatures. Future research work is needed to clarify such relationships through investigation of a wider range of compositions of the oligomers. The thermal analyses as well as the electrochemical measurement data indicated that the designed materials showed better thermal and oxidation stability than the corresponding **DH6T**. FET device tests suggest that these new oligomers are good candidates for stable electronic device applications. The emission color of these materials in the solid state ranging from green to red as well as their high mobilities may be useful features for organic laser applications.

The current study indicates that combining high and low band gap units in a conjugated oligomer is a promising approach for realizing high charge transport mobility and good device performance. The oligo(fluorene bithiophene) core studied here is such an example. It provides opportunities to easily vary its end substituents to further improve molecular order and solubility. In addition, some of the oligomers reported here appear to be thermotropic liquid crystals. It may be possible to align these oligomers from their liquid-crystal phase and achieve molecular orientation, which may lead to better performance in thin film electronic devices.

Experimental Section

General Methods. Chemical reagents were purchased from Aldrich Chemical Co. unless otherwise stated. All new compounds were characterized by mass spectrometry, elemental analysis (Robertson Microlit Laboratories), and ^{1}H NMR and ^{13}C NMR (due to the limited solubility of the new oligomers, their ^{13}C NMRs were not measured). Nuclear magnetic resonance (NMR) spectra were taken on a Bruker 360-MHz spectrometer unless otherwise stated. All chemical shifts were reported relative to tetramethylsilane (TMS) at 0.0 ppm. FTIR spectra were recorded on a Nicolet MAGNA-IR 560 spectrometer. UV−vis and fluorescence spectra were obtained on a HP-8453 spectrometer and a Spex Fluorolog-3 spectrofluorimeter, respectively. Thermogravimetric analysis (TGA) was carried out on a Perkin-Elmer TGA7 thermogravimetric analyzer at a heating rate of 10 °C/min and at a nitrogen flow rate of 75 cm^3/min. Differential scanning calorimetry (DSC) was run on a Perkin-Elmer DSC7 (differential scanning calorimetry) analyzer. Cyclic voltammetry (CV) was performed on a BAS 100B electrochemical analyzer with a three-electrode cell in a solution of 0.1 M tetrabutylammonium hexafluorophosphate (Bu$_4$NPF$_6$) dissolved in acetonitrile at a scan rate of 100 mV/ s. The oligomer thin films were coated on a platinum electrode (1.0 cm^2) by sublimation of the oligomer onto the electrode in

1786 *Chem. Mater., Vol. 15, No. 9, 2003*

Meng et al.

a vacuum (6×10^{-5} mbar). A Pt wire was used as the counter electrode and an Ag/AgNO$_3$ (0.1 M) electrode was used as the reference electrode. Its potential was corrected to the saturated calomel electrode (SCE) (0.31 V vs SCE) by measuring the ferrocene/ferrocenium couple in this system. The band gaps were derived either from the difference between onset potentials ($^{echem}E_g^{onset} = E_{pc}^{onset} - E_{na}^{onset}$) and/or measured according to the onset absorption of UV–vis–NIR ($^{opt}E_g^{onset} = 1240$ (nm)/ λ^{onset} (nm) eV. HOMO and LUMO energies were estimated by the empirical equation:[23] HOMO = 4.44 + E_{oxa}^{onset} (p-doping) and LUMO = 4.44 + E_{red}^{onset} (n-doping).

FET Device Fabrication. Both "bottom" and "top" contact configurations were used to make the FET devices similar to those previously reported in the literature.[25] The n-doped silicon substrate functions as the gate electrode. A 3000-Å silicon dioxide dielectric layer with a capacitance per unit area of 1.1×10^{-8} F/cm^2 was thermally grown on the gate substrate. For the bottom contact geometry, gold electrodes forming channels of 250-μm width (W) and 1.5–25-μm length (L) were photolithographically defined. The semiconductor layer was then deposited over the entire electrode/dielectric surface. For the alternative top contact geometry, gold electrodes were deposited after the semiconductor deposition by using shadow masks with W/L of ca. 13–14/1. The organic semiconductors were deposited at a rate of 2–3 Å/s under a pressure of ~2.0 $\times 10^{-6}$ Torr to a final thickness of 500 Å determined by a quartz crystal monitor. The substrate temperature during deposition was controlled by heating or cooling the copper block where the substrate was mounted. The electrical characteristics were obtained at room temperature in air using a 4145B Hewlett-Packard (HP) semiconductor parameter analyzer. For morphological characterizations, the materials were deposited onto carbon-coated electron microscope grids and Si/SiO$_2$ chips simultaneously with the FET devices. X-ray diffraction studies were performed on the chips in the reflection mode at 40 kV and 25 mA. A 2-kW Rigaku X-ray generator was used as a source of Ni-filtered Cu Kα radiation. The films on the grids, used for electron microscopy, were shadowed with Pt/C at tan^{-1} 0.5 and lightly carbon-coated in a vacuum evaporator before examination using a JEOL transmission electron microscope operated at 100 kV.

Materials Synthesis. *2-Hexyl-9H-fluorene.* A Grignard reagent of *n*-hexylmagnesium bromide (0.13 mol), prepared by the reaction of *n*-hexyl bromide (24.6 g, 0.15 mol) with Mg (3.84 g, 0.16 mol) in ether (300 mL), according to ref 26, was added dropwise into a solution of 2-bromo-9H-fluorene (25.0 g, 0.102 mol) in ether (250 mL) containing 1,3-bis(diphenylphosphino)-propane]dichloronickel(II) (Ni(dppp)$_2$Cl$_2$) (500 mg, 8 mmol) as a catalyst over a period of 1 h. After refluxing for 20 h, the reaction mixture was quenched with 0.2 M HCl and extracted with ether. The combined ether solution was washed with H$_2$O three times, followed by brine, and finally was dried over anhydrous MgSO$_4$. After removal of solvent, the resulting white powder was subjected to purification by flash chromatography using silica gel with hexane as the eluent. Recrystallization from methanol yielded white crystals (23.0 g, yield, 90%). mp 61.5–62.0 °C. MS (EI) *m/z*: 250 (M$^+$, 100). ^{1}H NMR (CDCl$_3$): δ_H 7.74 (d, $J = 7.45$ Hz, 1 H), 7.69 (d, $J = 7.74$ Hz, 1 H), 7.52 (d, $J = 7.38$ Hz, 1 H), 7.36–7.35 (m, 1 H), 7.35 (s, 1 H), 7.28–7.26 (m, 1H), 7.11 (d, $J = 7.70$ Hz, 1H), 3.92 (s, 2 H), 2.67 (t, $J = 7.76$ Hz, 2 H), 1.67–1.63 (m, 2 H), 1.38–1.29 (m, 18 H), 0.90 (t, 3 H) ppm. ^{13}C NMR (CDCl$_3$): δc 143.41, 143.10, 141.80, 139.30, 126.99, 126.61, 126.157, 125.03, 124.91, 119.53, 36.79, 36.15, 31.75, 29.02, 22.59, 14.07 ppm. Elemental anal. Found: C, 90.57; H, 8.49. Calcd for C$_{19}$H$_{22}$: C, 91.14; H, 8.86.

2-Bromo-7-hexyl-9H-fluorene. The synthesis of this compound is similar to that described in the literature for 2-bromo-

9H-fluorene.[27] A mixture of *N*-bromosuccinimide (NBS) (8.9 g, 0.05 mol) and 2-hexyl-9H-fluorene (12.5 g, 0.05 mol) in propylene carbonate (100 mL) was heated to 140 °C for 2 h, followed by stirring at room temperature overnight. The mixture was then poured into water (500 mL). The precipitate was filtered, washed with methanol, and dried in air. The crude product was subjected to flash chromatography using silica gel and using hexane as the eluent. Evaporation of the solvent results in 15.7 g of white crystals (yield, 95%). MS (EI) *m/z*: 328 (M$^+$, 100). ^{1}H NMR (CDCl$_3$): δ_H 7.64 (s, 1 H), 7.80 (d, $J = 7.60$ Hz, 1 H), 7.76 (d, $J = 7.60$ Hz, 1 H), 7.69 (d, $J = 7.60$ Hz, 1 H), 7.48 (s, 1 H), 7.17 (d, $J = 7.60$ Hz, 1 H), 3.84 (s, 2 H), 2.65 (t, $J = 7.56$ Hz, 2 H), 1.67–1.61 (m, 2 H), 1.35–1.28 (m, 18 H), 0.88 (t, 3 H) ppm. ^{13}C NMR (CDCl$_3$): δc 145.1, 143.1, 142.3, 140.8, 138.3, 129.8, 128.1, 127.2, 125.1, 120.8, 119.9, 119.6, 36.63, 36.14, 31.70, 31.71, 28.99, 22.58, 14.05 ppm. Elemental anal. Found: C, 68.97; H, 6.33. Calcd for C$_{19}$H$_{21}$Br: C, 69.30; H, 6.43.

2-(7-Hexyl-9H-fluoren-2-yl)-4,4,5,5-tetramethyl-1,3,2-dioxaborolane. A nitrogen-flushed three-neck round-bottom flask was charged with 2-bromo-7-hexyl-9H-fluorene (2.0 g, 6.1 mmol), bis(pinacolato)diboron (1.7 g, 6.7 mmol), potassium acetate (1.96 g, 20.0 mmol), and [1,1'-bis(diphenylphosphino)-ferrocene]dichloropalladium (0.16 g, 0.2 mmol), complex with dichloromethane (1:1). Dimethyl sulfoxide (DMSO, 40 mL) was then added and the mixture was bubbled with nitrogen for 15 min. After being heated at 80 °C for 16 h, the reaction mixture was cooled to room temperature and poured into ice water (200 mL). It was then extracted with diethyl ether (20 mL × 3) and the combined organic layer was dried over anhydrous magnesium sulfate. The solvent was removed by rotary evaporation and the residue was passed through a flash silica gel column with hexane:methylene chloride (v/v: 2:1) as the eluent to give white crystals (1.41 g, yield, 60%). mp: 74–75 °C. MS (EI) *m/z*: 376 (M$^+$, 100). ^{1}H NMR (CDCl$_3$): δ_H 7.95 (s, 1 H), 7.80 (d, $J = 7.60$ Hz, 1 H), 7.75 (d, $J = 7.60$ Hz, 1 H), 7.69 (d, $J = 7.60$ Hz, 1 H), 7.48 (s, 1 H), 7.17 (d, $J = 7.60$ Hz, 1 H), 3.84 (s, 2 H), 2.66 (t, $J = 7.56$ Hz, 2 H), 1.67–1.61 (m, 2 H), 1.35–1.28 (m, 18 H), 0.88 (t, 3 H) ppm. ^{13}C NMR (CDCl$_3$): δc 144.7, 144.1, 142.3, 139.2, 133.4, 131.1, 127.0, 125.0, 120.0, 118.8, 83.61, 36.58, 36.13, 31.66, 31.56, 28.93, 24.84, 22.48, 13.89 ppm. Elemental analy. Found: C, 78.64; H, 8.47; B, 3.09. Calcd for C$_{25}$H$_{33}$O$_2$B: C, 79.79; H, 8.84; B, 2.87.

*5,5′-Bis-(7-hexyl-9H-fluoren-2-yl)-2,2′-bithiophene (**DHFT-TF**).* To a solution of 2-(7-hexyl-9H-fluoren-2-yl)-4,4,5,5-tetramethyl-1,3,2-dioxaborolane (0.488 g, 1.3 mmol) and 2,2′-dibromobithiophene (0.162 g, 0.5 mmol) dissolved in toluene (5 mL) was added sodium carbonate (1.06 g, 10 mmol) dissolved in water (5 mL) followed by the addition of phase-transfer agent Aliquat 336 (0.4 g, 1.0 mmol). The mixture was bubbled with nitrogen for 15 min. Then, tetrakis(triphenylphosphine)palladium(0) (80 mg, 0.069 mmol) was added. The mixture was heated to 85 °C for 3 days under a nitrogen atmosphere. The reaction mixture was cooled to room temperature and poured into methanol (100 mL). The yellow precipitate was filtered off and washed with water and diluted acid (5% HCl), followed by water. The crude product was extracted with methanol overnight and then washed with hot acetone three times (60 mL × 3) to remove the starting material as well as the monosubstituted byproduct. The product was further purified by vacuum sublimation to give a yellow powder (0.26 g, yield, 79%). mp, decomposes before melts. MS (EI) *m/z*: 662 (M$^+$, 90), 331 (M$^+$/2, 100%). ^{1}H NMR (bromobenzene-d_5, 100 °C): δ_H 7.68 (d, $J = 7.87$ Hz, 2 H), 7.64 (s, 2 H), 7.62 (d, $J = 7.75$ Hz, 2 H), 7.60 (dd, $J = 7.87$, 1.50 Hz, 2 H), 7.30 (dd, $J = 7.75$ Hz, 1.50 Hz, 2 H), 7.27 (s, 2 H), 7.18 (d, $J = 3.65$ Hz, 2 H), 7.16 (d, $J = 3.65$, 2 H), 3.75 (s, 4 H), 2.68 (t, $J = 7.51$ Hz, 4 H), 1.67–1.61 (m, 4 H), 1.40–1.33 (m, 12 H), 0.88 (t, 6 H) ppm. ^{1}H NMR (500 MHz) (CDCl$_3$, 40 °C): δ_H 7.97 (s, 2H), 7.82 (d, $J = 6.90$ Hz, 2 H), 7.76 (d, $J = 6.90$ Hz, 2 H), 7.70 (d, $J = 6.65$ Hz, 2 H), 7.62 (d, $J = 6.65$, 2 H),

(25) Laquindanum, J. G.; Katz, H. E.; Lovinger, A. J. *J. Am. Chem. Soc.* **1998**, *120*, 664.

(26) Li, W.; Katz, H. E.; Lovinger, A. J.; Laquindanum, J. G. *Chem. Mater.* **1999**, *11*, 458.

(27) Ross, S. D.; Finkelstein, M.; Petersen, R. C. *J. Am. Chem. Soc.* **1958**, *80*, 4327.

7.39 (m, 4 H), 7.22 (d, $J = 6.90$ Hz, 2 H), 3.92 (s, 4 H), 2.68 (t, $J = 7.81$ Hz, 4 H), 1.69–1.60 (m, 4 H), 1.40–1.30 (m, 12 H), 0.89 (t, 6 H) ppm. Elemental anal. Found: C, 83.33; H, 6.99; S, 9.67. Calcd for $C_{46}H_{46}S_2$: C, 83.09; H, 6.73; S, 9.44.

The following compounds have been synthesized using the same procedures as for **DHFTTF**.

*2,5-Bis(7-hexyl-9H-fluoren-2-yl)thiophene (**DHFTF**).* Light yellow powder (yield, 74%). mp 394 °C. MS *m/z*: 580 (M+, 100). ^{1}H NMR (500 MHz) (CDCl$_3$, 40 °C): δ_H 7.90 (s, 2H), 7.82 (d, $J = 6.90$ Hz, 2 H), 7.75 (d, $J = 6.90$ Hz, 2 H), 7.71 (d, $J = 6.65$ Hz, 2 H), 7.62 (d, $J = 6.65$ Hz, 2 H), 7.40 (s, 2 H), 7.22 (d,, $J = 6.90$ Hz, 2 H), 4.41 (s, 4 H), 2.70 (t, $J = 7.80$ Hz, 4 H), 1.69–1.60 (m, 4 H), 1.40–1.30 (m, 12 H), 0.88 (t, 6 H) ppm. Elemental anal. Found: C, 84.72; H, 6.06; S, 7.05. Calcd for $C_{42}H_{44}S$: C, 86.84; H, 7.64; S, 5.52.

*5,5″-Bis(7-hexyl-9H-fluoren-2-yl)- -2,2′;5′,2″-terthiophene (**DHF3TF**).* Orange-yellow powder (yield, 65%). mp. decomposes before melts. MS *m/z*: 744 (M+, 100%). ^{1}H NMR (500 MHz) (CDCl$_3$, 40 °C): δ_H 7.76 (s, 2H), 7.74 (d, $J = 7.50$ Hz, 2 H), 7.62 (d, $J = 7.50$ Hz, 2 H), 7.38 (s, 2 H), 7.25 (d, $J = 3.50$, 2 H), 7.19 (d, $J = 7.50$ Hz, 2 H), 7.11 (d,, $J = 3.50$ Hz, 2 H), 6.97 (m, 2H), 3.92 (s, 4 H), 2.69 (t, $J = 7.81$ Hz, 4 H), 1.69–1.60 (m, 4 H), 1.40–1.29 (m, 12 H), 0.89 (t, 6 H) ppm. Elemental anal. Found: C, 80.02; H, 5.96; S, 13.07. Calcd for $C_{50}H_{48}S_3$: C, 80.60; H, 6.49; S, 12.91.

2-(7-Hexyl-9H-fluoren-2-yl)thiophene. A Grignard reagent of 2-thienylmagnesium bromide (0.05 mol), prepared by reaction of 2-bromothiophene (5.43 g, 0.034 mol) with Mg (0.88 g, 0.037 mol) in ether (100 mL) following procedures previously described,[28] was added dropwise into a solution of 2-bromo-7-hexyl-9H-fluorene (8.46 g, 0.026 mol) in THF (150 mL) containing 1,3-bis(diphenylphosphino)propanedichloronickel(II) (Ni(dppp)$_2$Cl$_2$) (216 mg, 3 mmol) as catalyst over a period of 1.5 h. After refluxing for 20 h, the reaction mixture was quenched with 2 M HCl and extracted with ether. The combined ether extract was washed with water (×3) and brine and then dried over anhydrous MgSO$_4$. After removal of solvent, a dark-brown liquid oil was obtained and was subjected to the purification by chromatography on silica gel using hexane as an eluent, followed by recrystallization from methanol to give light yellow crystals (7.68 g, yield 90%). mp: 179–180 °C. MS *m/z*: 332 (M+, 100). ^{1}H NMR (CDCl$_3$): δ_H 7.75 (s, 1 H), 7.71 (d, $J = 7.95$ Hz, 1 H), 7.67 (d, $J = 7.76$ Hz, 1 H), 7.61 (dd, $J = 7.95$ Hz, 0.80 Hz, 1 H), 7.36 (s, 1 H), 7.33 (d, $J = 3.32$ Hz, 1 H), 7.25 (dd, $J = 3.43$ Hz, 1 H), 7.19 (dd, $J = 7.76$ Hz, 1.60 Hz, 1 H), 7.08 (dd, $J = 3.43$ Hz, 3.32 Hz, 1 H), 3.89 (s, 2 H), 2.67 (t, $J = 7.50$ Hz, 2 H), 1.69–1.63 (m, 2 H), 1.38–1.30 (m, 6 H), 0.88 (t, 3 H) ppm. Elemental anal. Found: C, 82.27; H, 7.12; S, 9.41. Calcd for $C_{23}H_{24}S$: C, 83.08; H, 7.28; S, 9.64.

2-Bromo-5-(7-hexyl-9H-fluoren-2-yl)thiophene. This compound was synthesized according to the same procedure as the synthesis of 2-bromothiophene as previously described.[29]

A dry round-bottom flask was charged with 100 mL of a 1:1 mixture of chloroform and acetic acid, and 2-(7-hexyl-9H-fluoren-2-yl)thiophene (4.5 g, 13.6 mmol) was added. The mixture was then purged with nitrogen for 10 min. N-bromosuccinimide (NBS) (2.41 g, 13.6 mmol) was added in portions over a period of 0.5 h. During the addition, the temperature of the reaction mixture was maintained at 10 °C. The mixture was stirred at room temperature overnight and then extracted with chloroform. The extract was washed with water and dried over anhydrous MgSO$_4$. The solvent was removed by rotary evaporation. The residue was subject to chromatography on silica gel using hexane: methylene chloride (v/v: 1:1) as an eluent, followed by recrystallization from methanol to give light brown crystals (4.89 g, yield: 88%). mp: 214–216 °C. MS *m/z*: 410 (M+, 100). H NMR (CDC$_{l3}$): δ_H 7.71 (d, $J = 7.95$ Hz, 1 H), 7.67 (d, $J = 7.76$ Hz, 1 H), 7.67 (s, 1 H), 7.52 (dd, $J = 7.95$ Hz, 1.43 Hz, 1 H), 7.37 (s, 1 H), 7.20 (d, $J = 7.63$ Hz, 1 H), 7.08 (d, $J = 3.85$ Hz, 1 H), 7.04 (d, $J = 3.85$ Hz, 1 H), 3.89 (s, 2 H), 2.68 (t, $J = 7.50$ Hz, 2 H), 1.68–1.64 (m, 2 H), 1.39–1.31 (m, 6 H), 0.88 (t, 3 H) ppm. Elemental anal. Found: C, 66.86; H, 5.50; S, 7.83; Br, 19.00. Calcd for $C_{23}H_{23}SBr$: C, 67.15; H, 5.64; S, 7.79; Br, 19.42.

*5,5‴-Bis(7-hexyl-9H-fluoren-2-yl)-2,2′,5′,2″,5″,2‴-quaterthiophene (**DHF4TF**).* 2-Bromo-5-(7-hexyl-9H-fluoren-2-yl)thiophene (0.90 g, 2.2 mmol) and 5,5′-bis-tributylstannyl-2,2′-bithiophenyl (0.744 g, 1 mmol) was dissolved in DMF (50 mL). The solution was bubbled with nitrogen for 15 min. Then, tetrakis(triphenylphosphine)palladium(0) (50 mg, 0.04 mmol) was added. The mixture was heated to 85 °C for 24 h under a nitrogen atmosphere. The reaction mixture was cooled to room temperature before being poured into methanol (100 mL). The yellow precipitate was filtered and washed with water, diluted acid (5% HCl), and then again with water. The crude product was washed with methanol, acetone, and hot chloroform (60 mL × 3) and then extracted with acetone overnight to remove the starting material as well as the monosubstituted byproduct. The product was further purified by vacuum sublimation to give an orange-red powder (0.56 g, yield, 68%). mp, decomposes before melts. MS *m/z*: 826 (M+, 68). Elemental anal. Found: C, 78.05; H, 5.50; S, 15.50. Calcd for $C_{54}H_{50}S_4$: C, 78.40; H, 6.09; S, 15.51. ^{1}H NMR (500 MHz) (CDCl$_3$, 40 °C): δ_H 7.85–7.62 (m, 10 H), 7.38 (s, 2 H), 7.34 (s, 2H), 7.20 (m, 6 H), 3.92 (s, 4 H), 2.81 (t, $J = 7.81$ Hz, 4 H), 1.69–1.60 (m, 4 H), 1.40–1.29 (m, 12 H), 0.88 (t, 6 H) ppm.

(28) Van Pham, C.; Mark, H. B., Jr.; Zimmer, H. *Synth. Commun.* **1986**, *16*, 689.

(29) Meng, H.; Huang, W. *J. Org. Chem.* **2000**, *65*, 3894–3901.